Supporting Information for:

Computational metabolic engineering strategies for growth-coupled biofuel production by *Synechocystis*

Kiyan Shabestary and Paul Hudson

For following Supplementary files, see http://shabestary2016.sourceforge.net
A file of OptGene mutants and corresponding BPCY (.xls)
A MATLAB script containing: modifications to the model iJN678, all reactions for biofuel production, execution of OptKnock, and calculation of flux distributions
An SBML of updated iJN678
OptFlux files containing reaction subsets (A, B, and C) considered for OptGene

Supplemental Note 1: Tradeoffs between growth and production in simulated batch culture

In the identified mutant strains, fixed carbon is partitioned between biomass and biofuel and this partition will affect overall titers obtained from a starting culture. While a strictly-inducible biofuel strain is beneficial for laboratory studies, growth-coupled strains would be useful for industrial applications where large amounts of inducer or large liquid handling (for media switching) may be prohibitively expensive. To explore the biofuel/biomass tradeoff, we simulated growth and butanol production from mutant strains to estimate total titers from a typical batch culture. The starting cell density was "dilute," at 2 mg DCW/L (OD_{730}=0.01). At these low cell densities we assume that there is no shading of light and that cells are not carbon limited, so that growth rate is constant (steady-state) and maximal, and that cells produce butanol at the rate predicted by FBA. Simulated exponential cell growth curves under these assumptions were similar to those observed experimentally. Details on these calculations are provided in Supplementary. In the simulation, the M1 mutant culture accumulated 150 mg/L butanol after 4 days. By forcing flux through the soluble transhydrogenase reaction, the growth-coupling strength was altered. We re-computed the predicted 1-butanol titers after 4 days for various Sth fluxes (**Fig. S3**). The highest final titer after 4 days (200 mg/L) was predicted for a strain with weak growth-butanol coupling. This indicates that a severely restricted butanol envelope may not give highest titers in batch culture.

FBA calculations imply steady-state, which is assumed under constant growth rate. Titers can only be calculated for this time interval obtained using the following equation.

$$OD(t) = OD_0 \cdot e^{\mu t}$$

Cultures are started for a typical OD_0 value of 0.01 until they reach OD 5 corresponding to the start of the stationary phase. From that, a time interval in which growth is constant can be determined and used for titer calculations.

The productivity under constant growth was calculated as the integral of the specific productivity times the cell density over time as following:

$$P = \int_0^T r_p \cdot \alpha \cdot OD_0 \, e^{\mu t} \, dt = \frac{r_p}{\mu} \cdot \alpha \cdot OD_0 (e^{\mu T} - 1)$$

T is the final time of cultivation in hours, r_p the specific productivity in mmol/gCDW/h and α the conversion factor from OD to a concentration value gCDW/L (0.21 for shake flasks). During day 1, we assume no butanol production corresponding to the lag phase. Titers in Fig. S3 were calculated for 4 days to remain in the constant growth rate range.

Supplemental Note 2: Comparison between metabolic models

There are multiple variants of the *Synechocystis* GEM and developing intervention strategies in one GEM may not be effective in another. Our intervention strategies were derived using the iJN678 model (Nogales et al., 2012) which we updated with current literature. When we transferred the M1 knockouts to the GEM developed by Knoop et al (Knoop et al., 2013), coupling between biomass and butanol was lost and further knockouts were required to regain coupling. A main difference between the two models is a reversible transhydrogenase reaction in the model of Knoop et al. These must be disabled in order to achieve butanol coupling through the But_FER pathway since transhydrogenase provides an NADH valve to NADPH. However, due to a general abundance of NADPH relative to NADH, we expect net flux from the transhydrogenase reaction to lie toward NADH generation, which appears to be borne out in practice (Angermayr et al., 2012). However, the activity of the transhydrogenase (*slr1239* and *slr1434*) in cyanobacteria has not been demonstrated.

Alternative co-factor usage for several reactions leads to additional knockout targets. For example, glycerol 3-phosphate dehydrogenase (G3PD2) catalyzes the irreversible reduction of DHAP to glycerol 3-phosphate using NADH in both models. In iJN678, a reverse reaction is catalyzed by G3PD and re-generates DHAP by oxidizing glycerol 3-phosphate with FAD. Since FAD is a rather constrained metabolite, this potential "NADH burning" cycle between DHAP and glycerol 3-phosphate carries low flux and is not a knockout target. In the model of Knoop, G3PD uses plastiquinone (PQ) to oxidize glycerol 3-phosphate. The resultant PQH2 is in turned linked to many reactions such that PQH2 can be easily dissipated. Therefore, the irreversible G3PD2 catalyzed reaction in the model of Knoop becomes a knockout target to prevent an NADH "burning" cycle. The actual cofactor preferences of G3PD is not known, but has a Rossman-fold NAD(P)H/FAD binding domain (NCBI BLAST), suggesting that FAD could be a co-factor. In all, 2 additional reactions were targeted for knockout to achieve butanol-growth coupling in the model of Knoop et al. (**Table S5**).

Table S1: Abbreviations used

13DPG	1,3-diphosphoglycerate, 3-phospho-D-glyceroyl phosphate
2PG	2-phosphoglycerate, D-glycerate 2-phosphate
2PGlyc	2-phosphoglycolate
3HB	(R)-3-hydroxybutyryl-CoA
3PG	3-phosphoglycerate, D-glycerate 3-phosphate
α-KG	α-ketoglutarate, 2-oxoglutarate
AaCoA	acetoacetyl-CoA
Ac	acetate
AcACP	acetyl-ACP
Acald	acetaldehyde
AcCoA	acetyl-CoA
Actp	acetyl phosphate
Ala	L-alanine
ARTO	alternative respiratory terminal oxidase
CDP-ME	4-(cytidine 5'-diphospho)-2-C-methyl-D-erythritol
CDP-MEP	2-phospho-4-(cytidine 5'-diphospho)-2-C-methyl-D-erythritol
Cit	citrate
DHAP	dihydroxyacetone phosphate
DMAPP	dimethylallyl diphosphate
DXP	1-deoxy-D-xylulose 5-phosphate
E4P	D-erythrose 4-phosphate
EtOH	ethanol
F6P	D-fructose 6-phosphate
FBP	D-fructose 1,6-bisphosphate
Flv2/Flv4	flavodiiron proteins 2 & 4
Fum	fumarate
G1P	D-glucose 1-phosphate
G3P	D-glucose 3-phosphate
G6P	D-glucose 6-phosphate
GDP	geranyl diphosphate
Glu	L-glutamate
Gln	L-glutamine
HMBPP	1-hydroxy-2-methyl-2-(E)-butenyl 4-diphosphate
Icit	isocitrate
IPP	isopentenyl diphosphate
Lac	lactate
Mal	malate
MalCoA	malonyl-CoA
ME-cPP	2-C-methyl-D-erythritol 2,4-cyclodiphosphate
MEP	2-C-methyl-D-erythritol 4-phosphate
OcACP	octanoyl-ACP
PEP	phosphoenolpyruvate
PHB	polyhydroxybutyrate
PSP	3-phosphoserine phosphatase
PSTA	phosphoserine transaminase
Pyr	pyruvate
R5P	α-D-ribose 5-phosphate
Ru5P	D-ribulose 5-phosphate
RuBP	D-ribulose 1,5-bisphosphate
S17BP	sedoheptulose 1,7-bisphosphate
S7P	sedoheptulose 7-phosphate
Succ	succinate

Sucsal	succinic semialdehyde
SucCoA	succinyl-CoA
X5P	D-xylulose 5-phosphate

Abbreviations for reaction names used in iJN678 can be found in those authors supplementary files (Nogales et al., 2012; Dataset_S01)

Table S2. Reactions added to iJN678 according to current literature.

Modified iJN678			
Pathway	**Ref**	**Reaction**	**Modification**
SSDH shunt	Zhang and Bryant, 2011	SSDH_shunt	akg[c] -> sucsal[c] + co2[c]
		ABTA	Set to 0
FPK	Xiong et al., 2015	FPK	f6p[c] + pi[c] -> actp[c] + e4p[c] + h2o[c]
Serine	Klemke et al., 2015	PSTA	3php[c] + glu-L[c] -> 3ps[c] + oaa[c]
		PSP	3ps[c] -> ser-L[c] + pi[c]
ETC	Lea-Smith et al., 2015	NDH2_2p	h[c] + nadh[c] + pq[p] -> nad[c] + pqh2[p]
		ARTO	pqh2[p] + 0.5 o2[p] + 2 h[c] -> pq[p] + h2o[p]
		Flv2/Flv4	pqh2[u] + 0.5 o2[u] + 2 h[c] -> pq[u] + h2o[u]
		CBFCpp	Set to 0
		CBFC2pp	Set to 0
		CYO1b2pp_syn	Set to 0
		CYO1bpp_syn	Set to 0
		CYO1b2_syn	Set to 0
		NDH1_2p	Set to 0
		NDH1_1p	Set to 0

Table S3. Reactions added to iJN678 to create iJN678_But_FER, iJN678_Oct_FA, and iJN678_Limonene.

But_FER	
Enzyme(s)	*Reaction**
PhaA *(native)*	2 accoa[c] -> aacoa[c] + coa[c]
NphT7 (only present in variant)	mal-coa[c] + accoa[c] + atp[c] -> aacoa[c] + co2[c] + coa[c] + amp[c] + ppi[c]
PhaB *(native)*	h[c] + nadph[c] + aacoa[c] -> nadp[c] + 3hbcoa-R[c]
PhaJ	3hbcoa-R[c] -> crotonyl-coa[c] + h2o[c]
Ter	crotonyl-coa[c] + nadh[c] + h[c] -> butyryl-coa[c] + nad[c]
AdhE2 / Bldh	butyryl-coa[c] + nadh[c] + h[c] -> butyrald[c] + nad[c] + coa[c]
AdhE2 / YqhD	butyrald[c] + nadh[c] + h[c]-> 1-butanol[c] + nad[c]
Oct_FA	
Enzyme(s)	*Reaction*
Tes	octanyl-acp[c] + h2o[c] -> octanoate[c] + acp[c] + h[c]
Car	octanoate[c] + nadph[c] + h[c] + atp[c] -> octanal[c] + nadp[c] + amp[c] + ppi[c]
AdhA (*native*) / Ahr	octanal[c] + nadph[c] + h[c] -> 1-octanol[c] + nadp[c]
Limonene	
LS	grdp[c] -> limonene[c] + ppi[c]

*[c] cytoplasmic compartment in iJN678

Table S4. Reactions added to iJN678 for alkanes production.

AAR C8	ocACP + NADPH + H^+ -> octanal + $NADP^+$
ADO C8	octanal + 2 NADPH + 2 h^+ + o2 -> heptane + for + 2 $NADP^+$ + h2o

Table S5. Reaction KOs added to M1 to achieve coupling in the model of Knoop et al.

Reaction	Enzyme	Reaction	Locus
R507	Alanine dehydrogenase	L-Alanine + NAD^+ + H2O <=> Pyruvate + NH_3 + NADH + H^+	sll1682
R263	Glycerol 3-phosphate dehydrogenase	sn-Glycerol 3-phosphate + NAD^+ <=> Glycerone phosphate + NADH + H^+	slr1755

Table S6. Reaction KOs or upregulation for M4 mutant (limonene)

Reaction name in iJN678	Enzyme(s)	Reaction*	Locus to target**
NDH1_1u	NAD(P)H dehydrogenase NDH-1 (thylakoid)	4 h[c] + nadph[c] + pq[u] -> nadp[c] + 3 h[u] + pqh2[u]	*slr0331 (ndhD1) and slr1291 (ndhD2)*
NDH1_2u	NAD(P)H dehydrogenase NDH-1 (thylakoid)	4 h[c] + nadh[c] + pq[u] -> nad[c] + 3 h[u] + pqh2[u]	*slr0331 (ndhD1) and slr1291 (ndhD2)*
NDH2_syn	NdbA, NdbB, NdbC (thylakoid)	h[c] + nadh[c] + pq[u] -> nad[c] + pqh2[u]	*slr0851, slr1743, and sll1484*
NDH2_2p	NdbA, NdbB, NdbC (periplasm)	h[c] + nadh[c] + pq[p] -> nad[c] + pqh2[p]	*slr0851, slr1743, and sll1484*
NDH1_3u	Active CO2 transporter facilitator (thylakoid)	3 h[c] + h2o[c] + nadph[c] + pq[u] + co2[p] -> nadp[c] + hco3[c] +3 h[u] + pqh2[u]	*sll1733 (ndhD3) and sll0027 (ndhD4)*
NDH1_4pp	Active CO2 transporter facilitator (periplasm)	3 h[c] + h2o[c] + nadph[c] + pq[u] + co2[p] -> nadp[c] + hco3[c] +3 h[u] + pqh2[u]	*sll1733 (ndhD3) and sll0027 (ndhD4)*
Mehler	Flavodiiron proteins Flv1 and Flv3	h[c] + 0.5 o2[c] + nadph[c] -> h2o[c] + nadp[c]	*sll1521 (flv1), sll0550 (flv3)*
Cyo1b_syn	Cytochrome c oxidase	4 h[c] + 2 focytc6[u] + 0.5 o2[u] -> 2 h[u] + 2 ficytc6[u] + h2o[u]	*slr1137*
FQR	Cyclic Electron Flow	2 h[c] + pq[u] + 2 fdxr-2:2[c] -> pqh2[u] + 2 fdxo-2:2[c]	*ssr2016*
GLYCTO1	Glycolate oxidase	o2[c] + glyclt[c] -> h2o2[c] + glx[c]	*sll0404 (glcD2)*
GLUDy	Glutamate dehydrogenase (NADP)	h2o[c] + nadp[c] + glu-L[c] <=> h[c] + nadph[c] + akg[c] + nh4[c]	*slr0710*
ACKr	Acetate kinase	atp[c] + ac[c] <=> adp[c] + actp[c]	*sll1299*
H2ase_syn	[NiFe] Hydrogenase	h[c] + nadph[c] <=> nadp[c] + h2[c]	*sll1224 (hoxY)*
FPK	Phosphoketolase	f6p[c] + pi[c] -> actp[c] + e4p[c] + h2o[c]	*slr0453*
CYPHYS	Cyanophycin synthetase	2 atp[c] + asp-L[c] + arg-L[c] + precyanphy[c] -> 2 adp[c] + 2 h[c] + 2 pi[c] + cyanphy[c]	*slr2002*
NADTRHD	NAD transhydrogenase	nad[c] + nadph[c] <=> nadp[c] + nadh[c]	*slr1239 (pntA)*
ATPS4rpp****	ATP synthase (periplasmic)	3 adp[c] + 3 pi[c] + 14 h[p] -> 3 atp[c] + 11 h[c] + 3 h2o[c]	*slr1330 (atpE)*
PGK***	Phosphoglycerate kinase	atp[c] + 3pg[c] <=> adp[c] + 13dpg[c]	*slr0394*
PSII****	Photosystem II	2 h[c] + pq[u] + h2o[u] + 2 photon[c] -> 2 h[u] + pqh2[u] + 0.5 o2[u]	*slr0906 (psbB)*

*[c] cytoplasmic, [u] thylakoid, [p] periplasmic compartments.

**Locus to target is suggestion for gene deletion to eliminate enzyme activity. For multi-domain proteins a core subunit is given. NDH-1 (Battchikova, Eisenhut, & Aro, 2011), GlcD2 (Eisenhut et al., 2008), Hox (Eckert et al., 2012), AtpE (Imashimizu et al., 2011), PSII (Shen & Vermaas, 1994) .

***Overexpression required

****Downregulation required

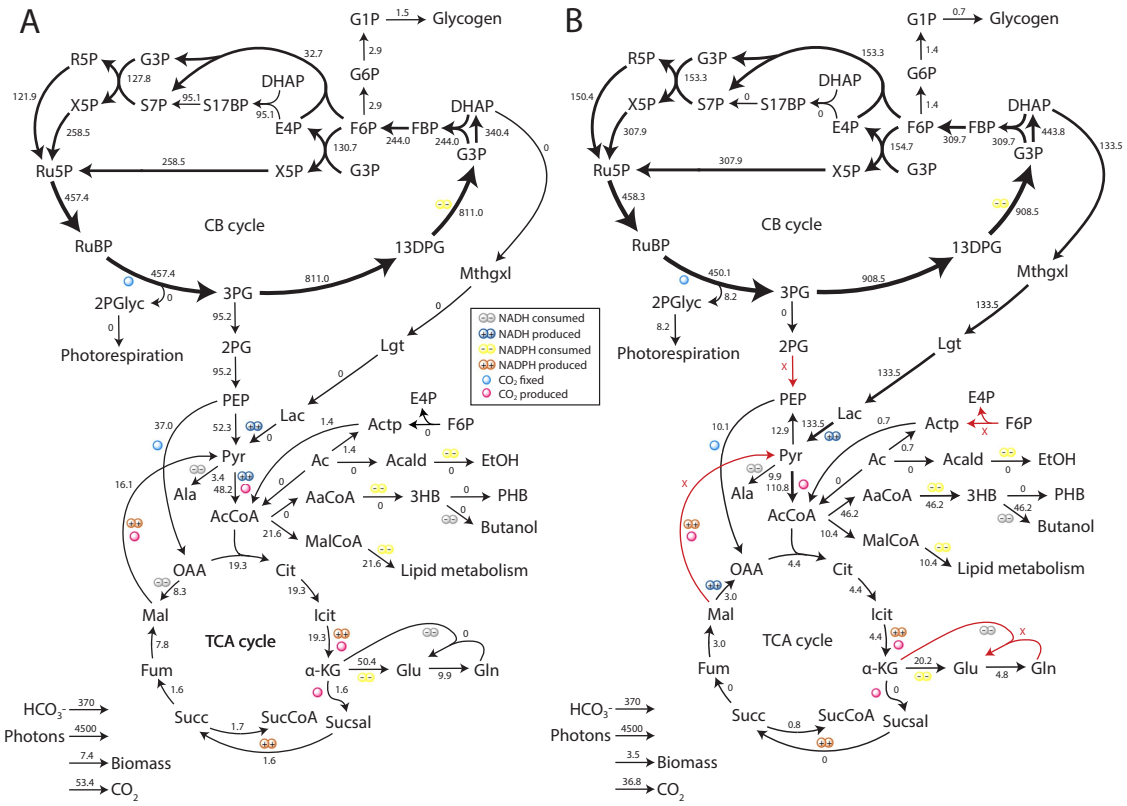

Fig. S1. Flux distributions of iJN678_ButFER and mutant M2. Fluxes were calculated using FBA with a biomass formation objective function in light-limited condition (see Methods). A) iJN678_But_FER, B) mutant M2**.** Flux values are in mmol/gDW.h (*10^{-2}).

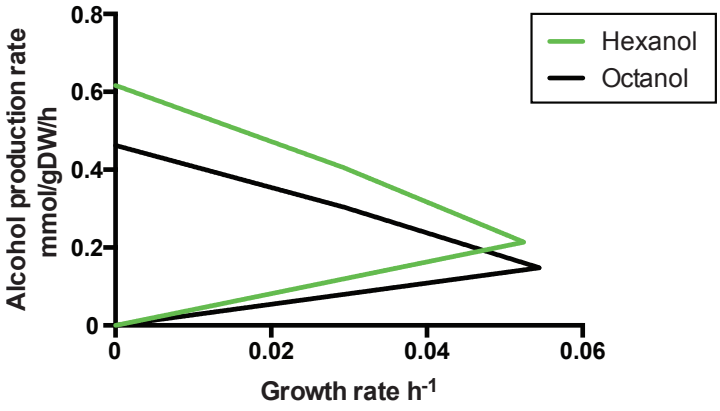

Fig. S2. Production envelope of *Synechocystis* iJN678 mutants. The respective reverse β-oxidation reactions were added (see MATLAB supplemental file) and the M1 reaction knockouts were applied.

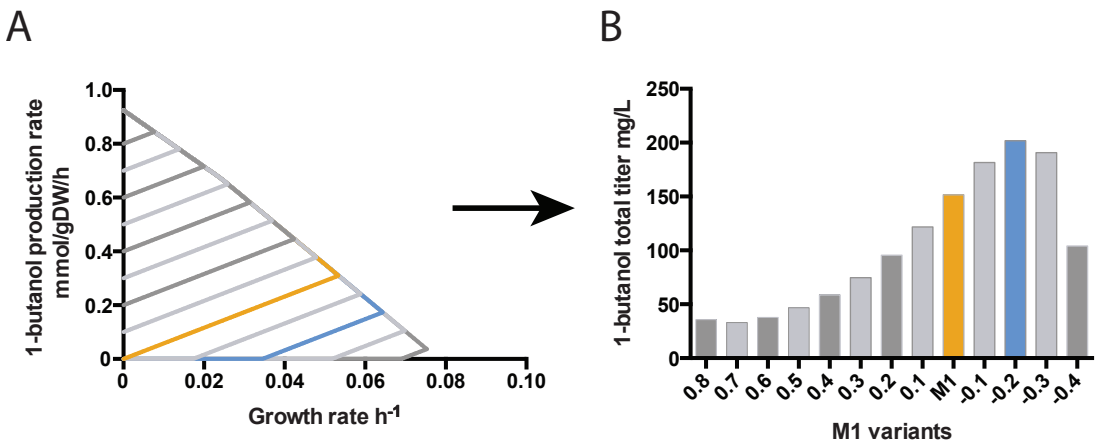

Fig. S3. Simulation of growth and butanol production of M1 variants. A) Production envelopes for fermentative butanol production by M1 and variants exhibiting forced flux through the Sth transhydrogenase reaction (NADPH + NAD^+ → NADH + $NADP^+$)**.** The M1 variant is in orange. B) Simulated butanol titers for M1 variants after 4 days of batch culture. Starting cell density was OD_{730}=0.01, approximately 2 mgDW/L. Variants are indicated by their forced flux through the Sth transhydrogenase reaction (mmol/gDW/hr). Note M1 mutant has no flux through this reaction.

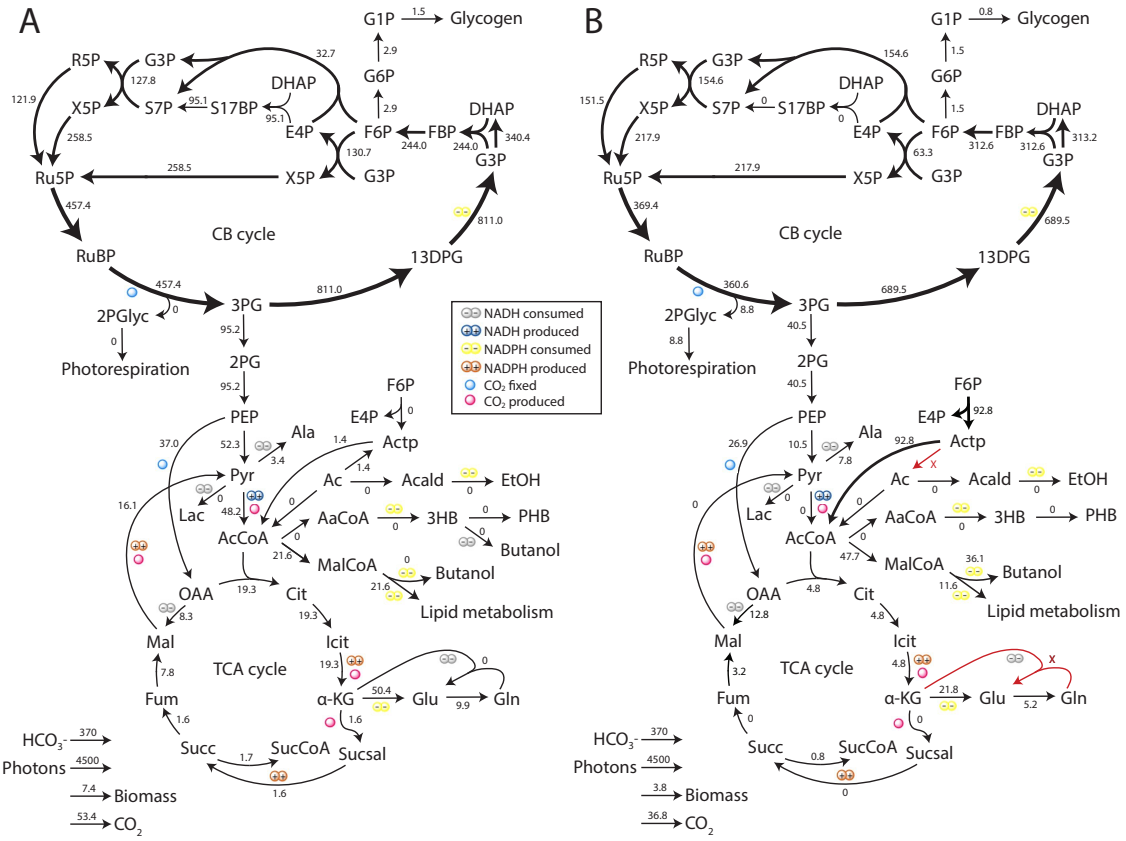

Fig. S4. Flux distributions between iJN678_ButFA and mutant M3. Fluxes were calculated using FBA with a biomass formation objective function in light-limited condition (see Methods). A) iJN678_ButFA, B) mutant M3**.** Flux values are in mmol/gDW.h (*10^{-2}).

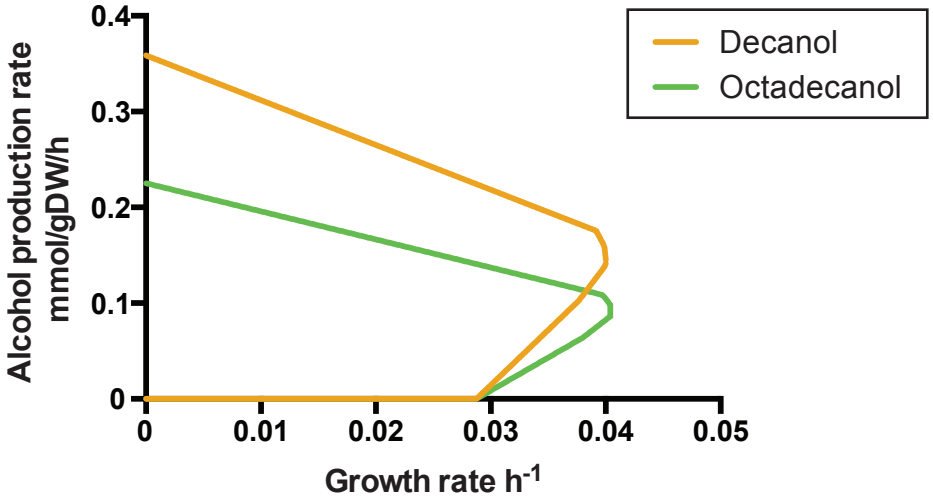

Fig. S5. Production envelope of *Synechocystis* iJN678 mutants and fatty alcohol production. The respective fatty alcohol reactions were added to the model (see supplemental MATLAB file). The M3 knockouts were applied.

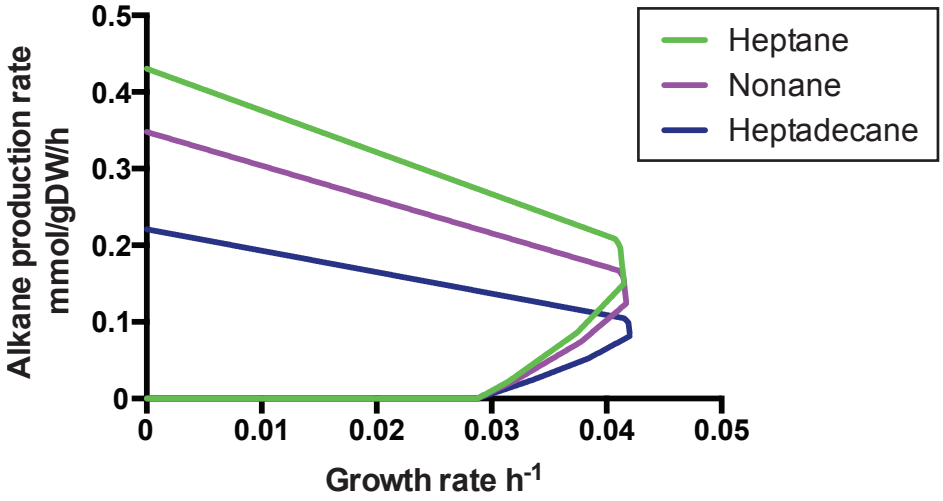

Fig. S6. Production envelope of *Synechocystis* iJN678 mutants and fatty alkane production. The respective fatty alcohol reactions were added to the model (see Supplemental MATLAB file). The M3 knockouts were applied.

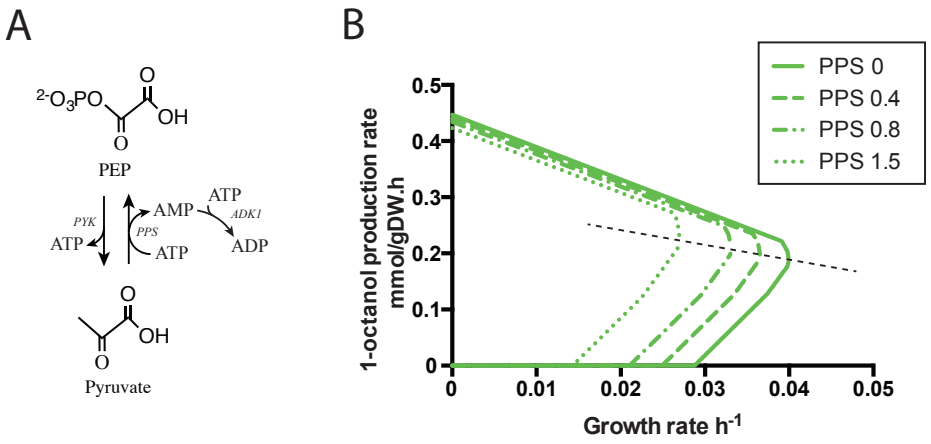

Fig. S7. *In silico* mutants that couple growth and 1-octanol production. A) A proposed futile cycle using PEP synthetase (PPS) in combination with pyruvate kinase (PYK) and adenylate kinase (ADK1) with a net consumption of one ATP. **B)** Forcing flux through the PPS reaction strengthens coupling in the M3 mutant.

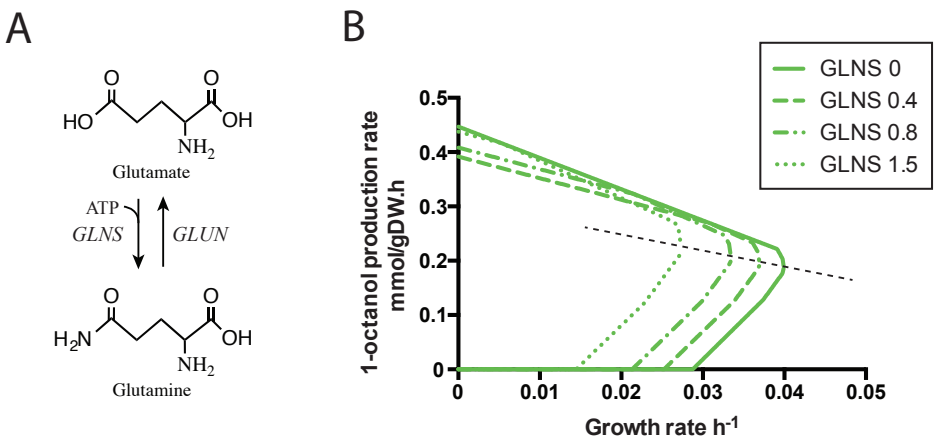

Fig. S8. *In silico* mutants that couple growth and 1-octanol production. A) A proposed futile cycle using glutamine synthase (GLNS) together with glutaminase (GLUN). **B)** Forcing flux through the GLNS reaction strengthens coupling in the M3 mutant.

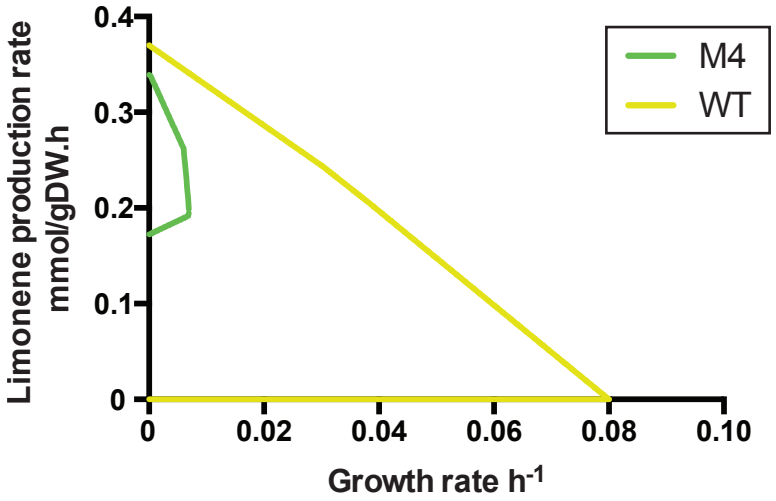

Fig. S9. Production envelope for M4 mutant. M4 mutant couples limonene to growth in iJN678_Limonene.

References

Angermayr, S. A., Paszota, M., & Hellingwerf, K. J. (2012). Engineering a cyanobacterial cell factory for production of lactic acid. *Applied and Environmental Microbiology*, *78*(19), 7098–106. http://doi.org/10.1128/AEM.01587-12

Battchikova, N., Eisenhut, M., & Aro, E. M. (2011). Cyanobacterial NDH-1 complexes: Novel insights and remaining puzzles. *Biochimica et Biophysica Acta - Bioenergetics*, *1807*(8), 935–944. http://doi.org/10.1016/j.bbabio.2010.10.017

Eckert, C., Boehm, M., Carrieri, D., Yu, J., Dubini, A., Nixon, P. J., & Maness, P. C. (2012). Genetic analysis of the Hox hydrogenase in the cyanobacterium Synechocystis sp. PCC 6803 reveals subunit roles in association, assembly, maturation, and function. *Journal of Biological Chemistry*, *287*(52), 43502–43515. http://doi.org/10.1074/jbc.M112.392407

Eisenhut, M., Ruth, W., Haimovich, M., Bauwe, H., Kaplan, A., & Hagemann, M. (2008). The photorespiratory glycolate metabolism is essential for cyanobacteria and might have been conveyed endosymbiontically to plants. *Proceedings of the National Academy of Sciences of the United States of America*, *105*(44), 17199–204. http://doi.org/10.1073/pnas.0807043105

Imashimizu, M., Bernát, G., Sunamura, E., Broekmans, M., Konno, H., Isato, K., … Hisabori, T. (2011). Regulation of F0F1-ATPase from Synechocystis sp. PCC 6803 by gamma and epsilon subunits is significant for light/dark adaptation. *The Journal of Biological Chemistry*, *286*(30), 26595–26602. http://doi.org/10.1074/jbc.M111.234138

Knoop, H., Gründel, M., Zilliges, Y., Lehmann, R., Hoffmann, S., Lockau, W., & Steuer, R. (2013). Flux balance analysis of cyanobacterial metabolism: the metabolic network of Synechocystis sp. PCC 6803. *PLoS Computational Biology*, *9*(6), e1003081. http://doi.org/10.1371/journal.pcbi.1003081

Nogales, J., Gudmundsson, S., Knight, E. M., Palsson, B. O., & Thiele, I. (2012). Detailing the optimality of photosynthesis in cyanobacteria through systems biology analysis. *Proceedings of the National Academy of Sciences of the United States of America*, *109*(7), 2678–83. http://doi.org/10.1073/pnas.1117907109

Shen, G., & Vermaas, W. F. J. (1994). Chlorophyll in a Synechocystis sp. PCC 6803 mutant without photosystem I and photosystem II core complexes: Evidence for peripheral antenna chlorophylls in cyanobacteria. *Journal of Biological Chemistry*, *269*(19), 13904–13910.